Pattern Recognition Letters 11 (1990) 811-829 December 1990

Automatic selection of object enhancement operator with quantitative justification based on fuzzy set theoretic measures

Malay K. KUNDU and Sankar K. PAL

Electronics & Communication Sciences Unit, Indian Statistical Institute, 203, Barrackpore Trunk Road, Calcutta 700035, India

Abstract: An algorithm for automatic selection of a nonlinear function appropriate for object enhancement of a given image is described. The algorithm does not need iterative visual interaction and prior knowledge of image statistics in order to select the transformation function for its optimal enhancement. A quantitative measure for evaluating enhancement quality has been provided based on fuzzy geometry. The concept of minimizing fuzziness (ambiguity) in both grayness and in spatial domain, as used by Pal and Rosenfeld [4], has been adopted. The selection criteria are further justified from the point of bounds of the membership function. The effectiveness of the algorithm is demonstrated for unimodal, multimodal and right skewed images when possible nonlinear transformation functions are taken into account.

Key words: Fuzzy geometry, object enhancement, grayness amgibuity, bounds.

1. Introduction

The purpose of image enhancement is to improve the picture quality, more specifically, to improve the quality for visual judgement of the picture. Most of the existing enhancement techniques are heuristic and problem dependent [1-3]. When an image is processed for visual interpretation, it is ultimately up to the viewers to judge its quality for a specific application and how well a particular method works. The process of evaluation of image quality therefore becomes subjective which makes the definition of a well processed image an elusive standard for comparison of algorithm performance. Again, it is customary to have an iterative process with human interaction in order to select an appropriate operator for obtaining such a desired processed output.

For example, let us consider the case of contrast enhancement using a nonlinear functional mapping. Not every kind of nonlinear function will produce a desired (meaningful) enhanced version [2, pp. 10-13]. The questions that automatically arise are "Given an arbitrary image which type of nonlinear functional form will be best suited without prior knowledge on image statistics (e.g., in robot vision and remote applications where frequent human interaction is not possible) for highlighting its object?" and "Knowing the enhancement function how can one quantify the enhancement quality for obtaining the optimal one?". Regarding the first question, even if we are given the image statistics, it is possible only to estimate approximately the function required for enhancement and the selection of the exact functional form still needs human interaction in an iterative process. The second question, on the other hand, needs individual judgement which makes the optimal decision subjective.

The present work is an attempt to demonstrate

an application of the theory of fuzzy sets to avoid such human iterative interaction and to make the task of subjective evaluation objective. An algorithm is formulated here which minimizes (optimizes) two types of ambiguity (fuzziness), namely, ambiguity in grayness and ambiguity in geometry of an image containing an object.

It is to be mentioned here that the said ambiguity measures have been found recently by Pal and Rosenfeld [4] to obtain both fuzzy and nonfuzzy optimum segmentation for object-background classification of an image. Their algorithm used Zadeh's standard S-function [5] to compute the 'bright image' membership plane and to compute its ambiguities. By changing the cross-over point of the S-function for a fixed bandwidth, an optimum membership plane for which ambiguity is minimum was obtained.

The proposed algorithm has three parts. Given an input image X and a set of nonlinear transformation functions, it first of all enhances the image with a particular enhancement function with its varying parameters. The second phase consists of measuring both spatial ambiguity and grayness ambiguity of the various enhanced X' using the algorithm in [4], and of checking if these measures posses any valley (minimum) with change in the parameters. The same procedure is repeated in the third stage for other functions. Among all the valleys, the global one is selected. The corresponding function with the prescribed parameter values can be regarded as optimal, and the value of ambiguity corresponding to the global minimum can be viewed as a quantitative measure of enhancement quality.

The nature of nonlinearity of the optimal enhancement function is further justified from the point of bounds [7] of S-type membership functions. The effectiveness of the algorithm is demonstrated on various unimodal, bimodal, skewed and multimodal images when different nonlinear functions are considered as enhancement operators.

It is further to be noted that although the geometrical ambiguity measure [4] was formulated only for a single compact object, the present experiment has been extended to other types of objects also to investigate the effect of the said ambiguity measure.

2. Grayness ambiguity and spatial ambiguity [4]

A gray tone image X of L levels and dimension $M \times N$ can be considered as an array of fuzzy singletons, each having a value of membership denoting its degree of brightness relative to some brightness level l; $l = 0, 1, 2, \ldots, L-1$. In the notation of fuzzy sets, it can be represented as

$$X = \{(\mu(x_{mn}), x_{mn}) = \mu_{mn}/x_{mn}: \quad m = 1, 2, \ldots, M;\ n = 1, 2, \ldots, N\} \tag{1}$$

where x_{mn} is the (m, n)th pixel intensity, $0 \leqslant x_{mn} \leqslant L-1$. μ_{mn} $(= \mu(x_{mn}))$ denotes the grade of possessing some property (e.g., brightness, darkness, edginess, smoothness) by the (m, n)th pixel intensity x_{mn}.

The entropy of image X may be computed as

$$H(X) = \frac{1}{MN \ln 2} \sum_l T_e(l)\, h(l) \tag{2}$$

with

$$T_e(l) = -\mu(l) \ln \mu(l) - (1-\mu(l)) \ln(1-\mu(l))$$

and $h(l)$ denoting the frequency of level l.

Similarly, the area, perimeter and compactness of X [6] may be computed as

$$a(X) = \sum_m \sum_n \mu_{mn} = \sum_l \mu(l)\, h(l), \tag{3}$$

$$p(X) = \sum_{m=1}^{M} \sum_{n=1}^{N-1} |\mu_{mn} - \mu_{m,n+1}| + \sum_{n=1}^{N} \sum_{m=1}^{M-1} |\mu_{mn} - \mu_{m+1,n}|, \tag{4}$$

$$\text{comp}(X) = a(X)/p^2(X). \tag{5}$$

It is thus seen from the above measures that $H(X)$ considers global information and provides an average amount of fuzziness in grayness of X, i.e., the degree of difficulty (ambiguity) in deciding whether a pixel would be treated as black (dark) or white (bright). The difficulty is minimum when $\mu_{mn} = 0$ or 1 (i.e., the image is crisp with either fully black or white pixels) and maximum when $\mu_{mn} = 0.5$ (semi-bright pixels). Other grayness ambiguity measures, e.g., index of fuzziness and index of crispness are available in [4].

The measure comp(X), on the other hand, takes into account the local information and reflects an amount of fuzziness in geometry (spatial domain) of X. Among all possible fuzzy disks, the compactness is the smallest for its crisp version.

Combining the two types of ambiguity described above a composite measure was defined as

$$\theta(X) = H(X) \cdot \text{comp(X)} \tag{6}$$

which involves fuzziness both in gray level and in spatial domain of the image. Thus, a μ_{mn} plane having minimum θ value implies that the image X has minimum ambiguity (fuzziness) as far as the grayness and geometry of its object together are concerned.

For computing the ambiguity measures (equations (2)–(5)) of an image X, μ_{mn} is considered here to be a 'bright image' subset and is obtained from x_{mn} using Zadeh's standard S-function [7] as follows:

$$\begin{aligned}
\mu_{mn} &= 0, && x_{mn} \leqslant a, \\
&= 2\left(\frac{x_{mn}-a}{c-a}\right)^2, && a \leqslant x_{mn} \leqslant b, \\
&= 1-2\left(\frac{x_{mn}-c}{c-a}\right)^2, && b \leqslant x_{mn} \leqslant c, \\
&= 1 && x_{mn} \leqslant c
\end{aligned} \tag{7}$$

where $b = (a+c)/2$ is the cross-over point, i.e., at $x_{mn} = b$, $\mu_{mn}(x_{mn}) = 0.5$ and $.1b = b - a - c$ b is the bandwidth. μ_{mn} represents the degree of brightness of the (m,n)th pixel intensity x_{mn}.

3. Gray level rescaling

The gray level rescaling is one of the most widely used techniques for contrast enhancement which decreases the blurring and at the same time reveals the features of interest. Each pixel is directly requantized or mapped here to a new gray level in order to improve the contrast of the image. In many pictures, the gray level difference between object and background is so small that it becomes visually difficult to discriminate them; enhancement is then required to increase such difference.

The simplest form of the functional mapping may be expressed as

$$x'_{mn} = x_{\max} \cdot f(x_{mn})$$

where

x_{mn} = gray value of the (m,n)th pixel in the input image (original),

x'_{mn} = transformed gray vlaue of the (m,n)th pixel (enhanced),

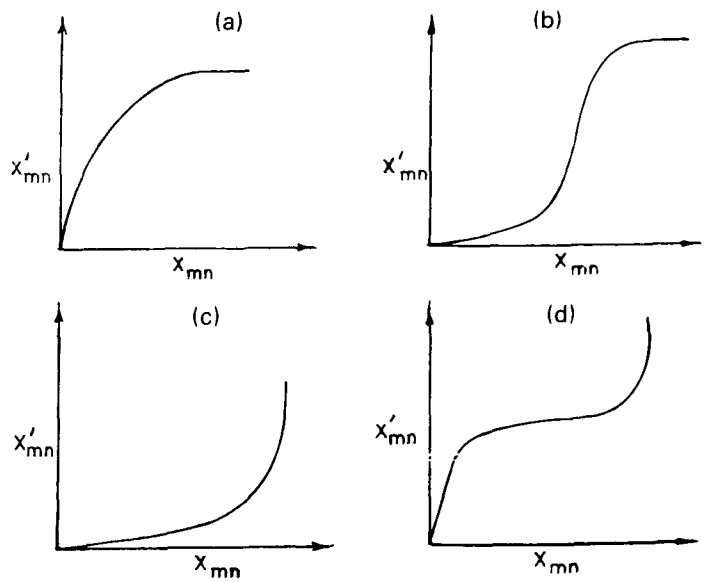

Figure 1. Commonly used mapping functions for image contrast enhancement.

$f(x_{mn})$ = prespecified transformation function, $0 \leqslant f \leqslant 1$,

x_{max} = maximum gray level of input dynamic range.

Some of the most popular [3] mapping functions are shown in Figure 1.

The transformation function like Figure 1(a) when applied on an image, makes the dark area (lower range of gray level) stretched and the bright area compressed, resulting in an increase in the contrast within the darker area of the image. Similarly, the application of a mapping function like Figure 1(c) will produce effects exactly opposite to that of Figure 1(a).

The mapping function as in Figure 1(b) will result in stretching of the middle range gray levels. The curve in Figure 1(d) (which is also known as gamma correcting curve for display of nonlinearity), when used as mapping function, will compress drastically the midrange values, and at the same time it will stretch the gray levels of the upper and lower ends.

In our experiment we have simulated these mapping operators with the help of different nonlinear functions in order to investigate their relative en-

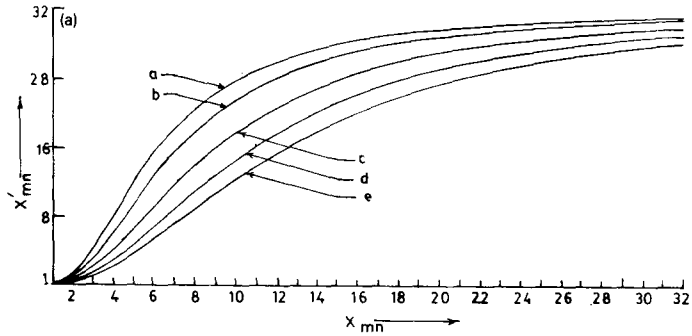

Figure 2(a). The mapping function corresponding to equation (8). a: $k=100$, b: $k=66.6$, c: $k=50$, d: $k=40$, e: $k=33.3$.

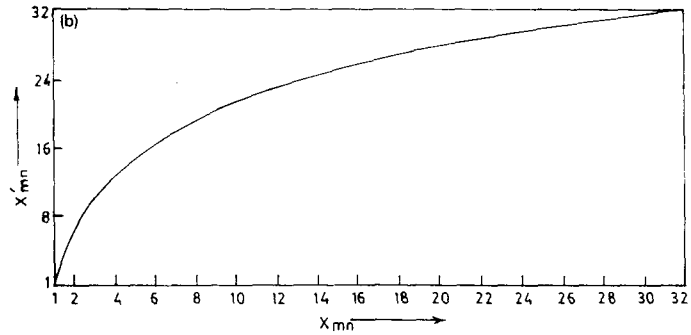

Figure 2(b). The mapping function corresponding to equation (9).

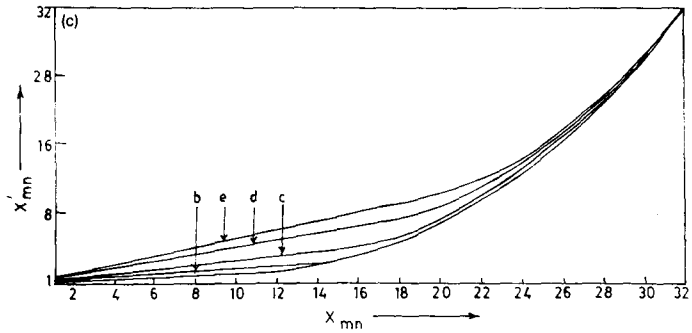

Figure 2(c). The mapping function corresponding to equation (10). a: $A=0.064$, $B=0.1$, $D=11$. b: $A=0.074$, $B=0.15$, $D=13$. c: $A=0.080$, $B=0.25$, $D=15$. d: $A=0.084$, $B=0.4$, $D=17$. e: $A=0.093$, $B=0.5$, $D=19$.

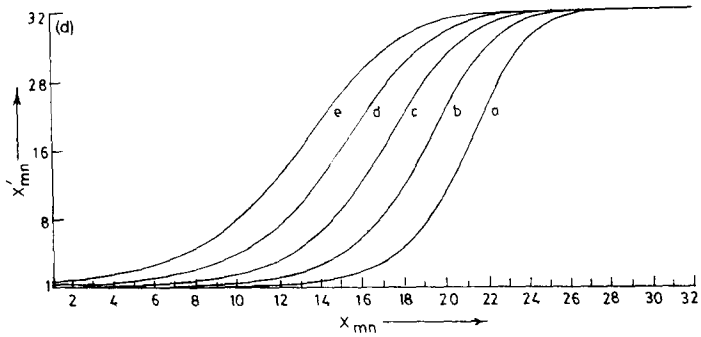

Figure 2(d). The mapping function corresponding to equation (11). a: $F_d = 12$, b: $F_d = 14$, c: $F_d = 16$, d: $F_d = 18$, e: $F_d = 20$.

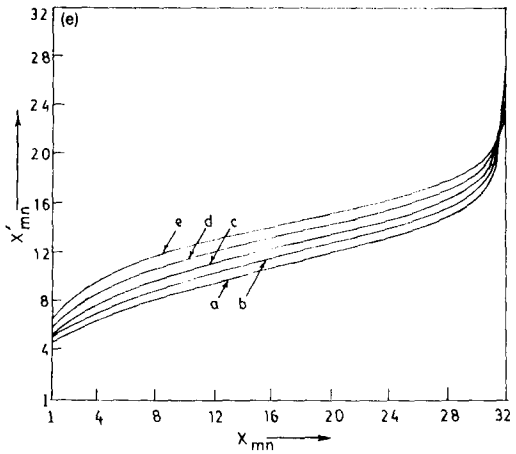

Figure 2(e). The mapping function corresponding to equation (12). a: $F_d = 22$, b: $F_d = 21$, c: $F_d = 20$, d: $F_d = 19$, e: $F_d = 18$.

hancement performance on different images. The following forms of nonlinear function (monotonically nondecreasing) are used to represent (approximately) the curves in Figure 1. The mapping function in Figure 1(a) is represented by either

$$f(x_{mn}) = \frac{ax_{mn}^2}{1+ax_{mn}^2} = \frac{x_{mn}^2}{1/a+x_{mn}^2} = \frac{x_{mn}^2}{k+x_{mn}^2} \tag{8}$$

or,

$$f(x_{mn}) = b\log(x_{mn}) \tag{9}$$

where the parameters a and b are positive constants.

The mapping function in Figure 1(c) is represented as

$$f(x_{mn}) = A[F(x_{mn})]^2 + Bx_{mn} + C$$
$$0 < A, B, C < 1 \tag{10}$$

where

$$F(x_{mn}) = x_{mn} - D \quad \text{for } x_{mn} > D,$$
$$= 0 \quad \text{for } x_{mn} \leqslant D,$$
$$x_{\min} < D < x_{\max}$$

where $x_{\min}$ and $x_{\max}$ are the minimum and maximum gray levels in the image.

The function in Figure 1(b) can be expressed as

$$f(x_{mn}) = \left[1 + \left(\frac{x_{\max} - x_{mn}}{F_d}\right)^{F_e}\right]^{-1} \tag{11}$$

and that of Figure 1(d) as

$$f(x_{mn}) = \frac{1}{x_{\max}}\left[x_{\max} - F_d\left\{\left(\frac{x_{\max}}{x_{mn}} + \beta\right) - 1\right\}^{-F_e}\right] \tag{12}$$

where F_e and F_d are positive constants and β is the value of $f(x_{mn})$ for $x_{mn} = 0$. The functional forms for equations (8)–(12) are shown through Figures 2(a)–2(e) respectively.

4. Algorithm

The block diagram of the proposed algorithm is shown in Figure 18 at the end of the paper. Given an input image X, it is first of all transformed (enhanced) by one of the nonlinear mapping functions f_i^q (Figures 2(a)–2(e)). The μ values of the transformed image X' are computed with Zadeh's standard S-function (equation (7)) in order to compute its $I(X')$ value. Here I stands for either entropy (equation (2)) or compactness (equation (5)) or θ (equation (6)). The same procedure is repeated for different parameters q of the function f_i^q. It is

then checked whether these ambiguity measures possess any valley or not.

A similar checking is adopted for other mapping functions under consideration. In the final stage, a global minimum (valley) is determined. The corresponding mapping function with specific q value can be regarded as optimum enhancement function of the image X. The image $X' = f_i^q(x_{mn})$ thus provides the optimum enhanced output, given a set of functions. The concept of optimum enhancement is explained below.

Concept of optimum fuzziness and object enhancement

Let us consider, for example, an image X consisting of an object in a background. An enhancement transformation (viz. equations (8)–(12)) when applied on X, attempts to enlarge the gaps in levels between two regions and at the same time to reduce the difference in levels within a region. As a result, the μ_{mn} values of the enhanced image would tend to either 0 or 1; thus making a decrease in value of $H(X)$.

It is to be noted that the above decrease in $H(X)$ (fuzziness in grayness) does not ensure proper enhancement of the object. In other words, unless the transformation function is able to discriminate the object geometry (or boundary) from the background, the $H(X)$ values even if they decrease will not reflect its meaningful enhancement. This leads one to determine the appropriate functional form such that the corresponding enhanced image would result in a minimum number of pixels having $\mu_{mn} \simeq 0.5$ and a maximum number of pixels with $\mu_{mn} \simeq 0$ or 1; thus contributing least (minimum) to $H(X)$. This may be treated as the optimum value of gray level fuzziness in the sense that the value obtained from any other transformation function will be greater than this.

Similar is the case with the spatial ambiguity measure comp(X) where modification of the enhancement function will result in different μ_{mn} planes with varying 'compactness'. comp(X) will reach a valley (optimum) only when there is an appropriate enhancement of the object geometry of X. For any other choices of enhancement function, either a part of the object will be treated as background or a part of the background will merge with the object. In the former case, both area and perimeter will decrease but the decrease is more for the denominator; thus resulting in a value greater than the optimum one. The latter case, on the other hand, involves faster increase of the numerator than that of the denominator and gives rise to the same result as the former one.

5. Bounds of membership function

All the enhancement functions $f(x_{mn})$ (equations (8)–(12)) are seen to be monotonically non-decreasing and $f(x_{mn}) \in [0, 1]$. These mapping functions $f(x_{mn})$ may therefore be viewed, like equation (7), as S-type membership functions μ_{mn} $(1 \geqslant \mu_{mn} \geqslant 0)$ for extracting a fuzzy subset 'bright image' from an image X. Recently, Murthy and Pal [7] formulated two bounds for S-type membership functions in order to select the membership functional forms which are preferably to be used while representing a fuzzy set in practice. The significance of these bounds in image segmentation and analysis problems was also found to be justified [7]. The optimum enhancement functions of an image obtained in the previous section may therefore be further judged with these bounds.

The expressions for bound functions are based on the properties of correlation [8] between two membership functions $\mu_1(x)$ and $\mu_2(x)$. The main properties on which correlation was formulated are:

P_1: If for higher values of μ_1, μ_2 takes higher values and the converse is also true, then the correlation $C_{\mu_1,\mu_2} > 0$.

P_2: If $\mu_1 \uparrow$ and $\mu_2 \uparrow$, then $C_{\mu_1,\mu_2} > 0$.

P_3: If $\mu_1 \uparrow$ and $\mu_2 \downarrow$, then $C_{\mu_1,\mu_2} < 0$.

($\uparrow$ denotes increases and $\downarrow$ denotes decreases.)

It is to be mentioned that P_2 and P_3 should not be considered in isolation of P_1. Had this not been considered, one can cite several examples when $\mu_1 \uparrow$ and $\mu_2 \uparrow$ but $C_{\mu_1,\mu_2} < 0$, and when $\mu_1 \uparrow$ and $\mu_2 \downarrow$ but $C_{\mu_1,\mu_2} > 0$. Subsequently, the type of membership functions which should not be considered in fuzzy set theory are classified with the help of correlation. Bound functions h and g for an S-function μ were accordingly derived as [7]:

$$h(x) = 0, \quad 0 \leqslant x \leqslant \delta,$$
$$= x - \delta, \quad \delta \leqslant x \leqslant 1, \tag{13}$$
$$g(x) = x + \delta, \quad 0 \leqslant x \leqslant 1 - \delta,$$
$$= 1, \quad 1 - \delta \leqslant x \leqslant 1 \tag{14}$$

where

$$x \in [0, 1], \quad \delta \simeq 0.25.$$

The bounds are such that

$$C_{h,g} > 0, \quad C_{h,\mu} \geqslant 0, \quad C_{g,\mu} \geqslant 0, \quad h \leqslant \mu \leqslant g. \tag{15}$$

A function μ satisfying these bounds does not have most of its variation concentrated on a small interval of $[0, 1]$. For any arbitrary interval $[a, b]$, the bound functions will change proportionately according to the length of interval.

In the light of object-backgroud classification (or contrast enhancement), the interpretation of these bounds is that the membership function which best represents the fuzziness in gray level of an image must have values $\simeq 0.5$ over the ambiguous (around threshold) gray levels.

Since the enhancement functions are viewed as S-type membership functions, the equations (13)–(15) may thus be used to see whether the optimum enhancement function of an image satisfies the bound criteria.

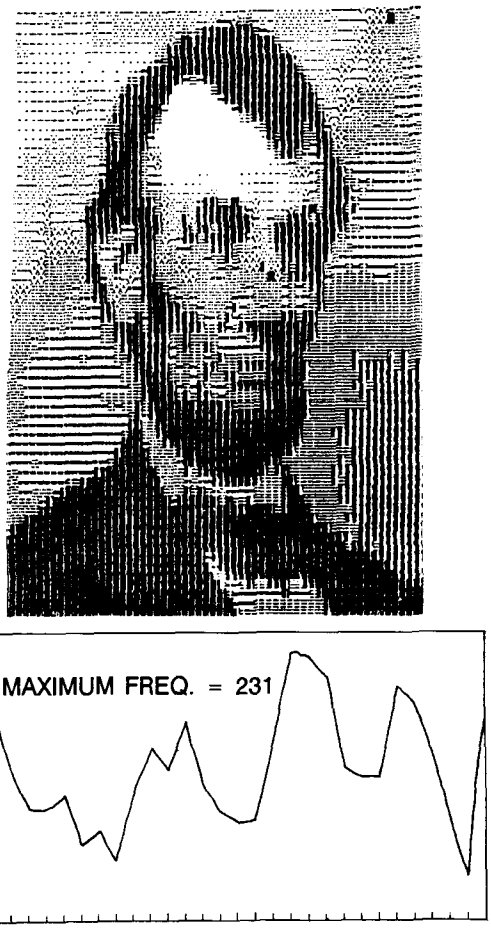

Figure 3. Lincoln image and its gray level histogram.

6. Results

To study the effects of various types of enhancement (mapping) function on different types of images, we have considered here four different types of image namely, Lincoln, Chromosome, Cell and Biplane which have multimodal, highly right skewed, partially skewed and bimodal histograms as shown in Figures 3–6. The different mapping (enhancement) functions indicated by equations (8), (10), (11) and (12) and their varying forms (for different values of parameters) were applied on each image. For every form of the mapping functions the three different fuzzy set theoretic measures such as entropy ($H(X)$), entropy-compactness product ($\theta(X)$) and compactness (comp(X)) were calculated using the

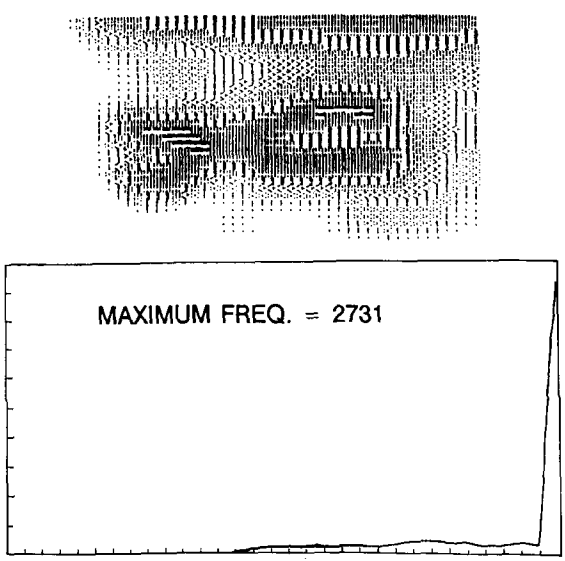

Figure 4. Chromosome image and its gray level histogram.

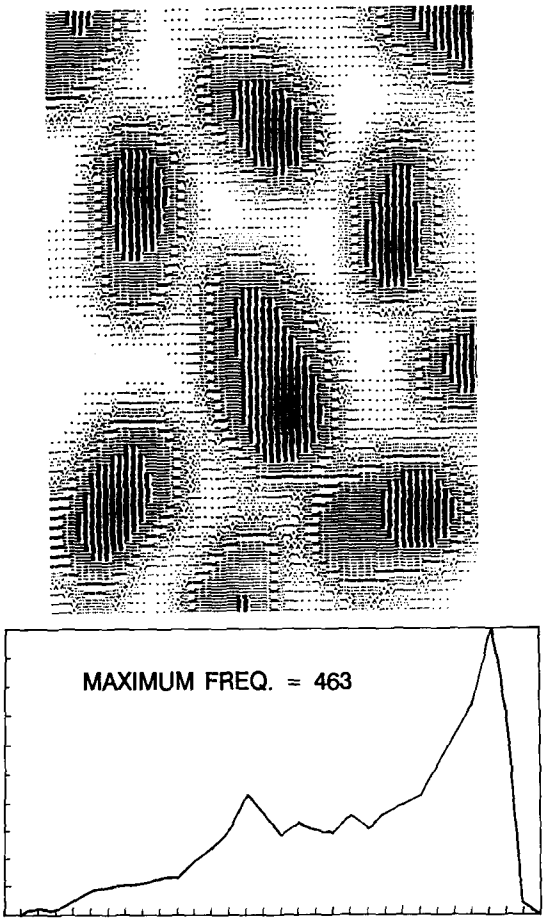

Figure 5. Cell image and its gray level histogram.

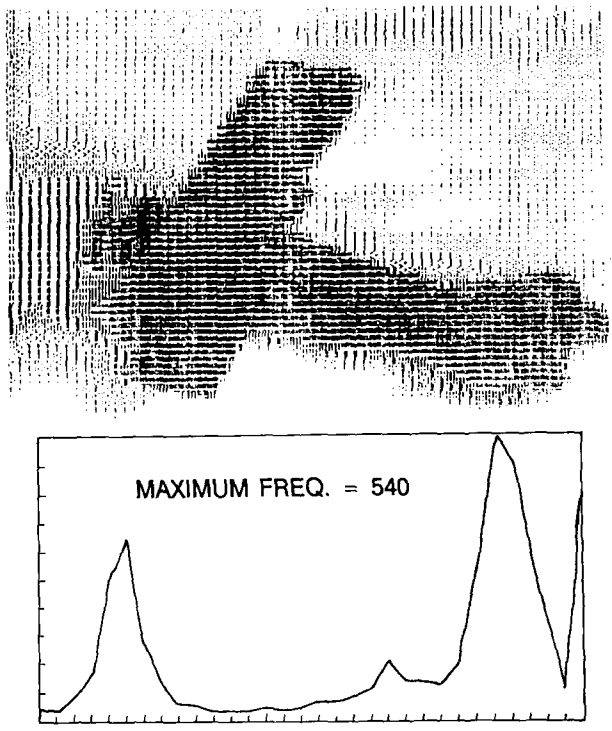

Figure 6. Biplane image and its gray level histogram.

algorithms described in Section 2. Table 1 shows the values of these measures for the input images. The programs were simulated on a PDP-11/24 microcomputer system. The dot matrix printer was used to produce hard copy of the images, where various gray levels of the image were represented by different graphic patterns.

Figures 7(a)–(d) show plots of H and θ for various values of a in equation (8), corresponding to the images of Lincoln, Chromosome, Cell and Biplane. Figure 8 gives the variation of comp(X) of these images separately. Both $H(X)$ and $\theta(X)$ are found to decrease monotonically in Figures 7(b) and 7(c), and to increase monotonically in Figure 7(d) with a. Whereas, in Figure 7(a) it is seen for the Lincoln image that θ increases while H decreases with a. From these plots we can infer that in the cases of Figures 7(b) and 7(c) as a increases there will be some quality enhancement effect (decrease in ambiguity in grayness and perhaps in spatial domain) for the Chromosome and Cell images. For the Biplane image, there is no such reduction in ambiguity considering either H or θ as a increases. But considering their 'comp' measure (Figure 8), we see that there are valleys at $a=0.015$ and $a=0.025$ indicating optimal enhancement of the Biplane and Chromosome images as far as their fuzziness in geometry alone is concerned. The enhancement is optimal in the

Table 1
Ambiguity measures for different input images

Image	Entropy (H)	Compactness (comp)	Product of H and comp (θ)
Lincoln	0.481	0.00428	0.00128
Chromosome	0.175	0.0892	0.00988
Cell	0.141	0.014	0.00484
Biplane	0.304	0.0150	0.00219

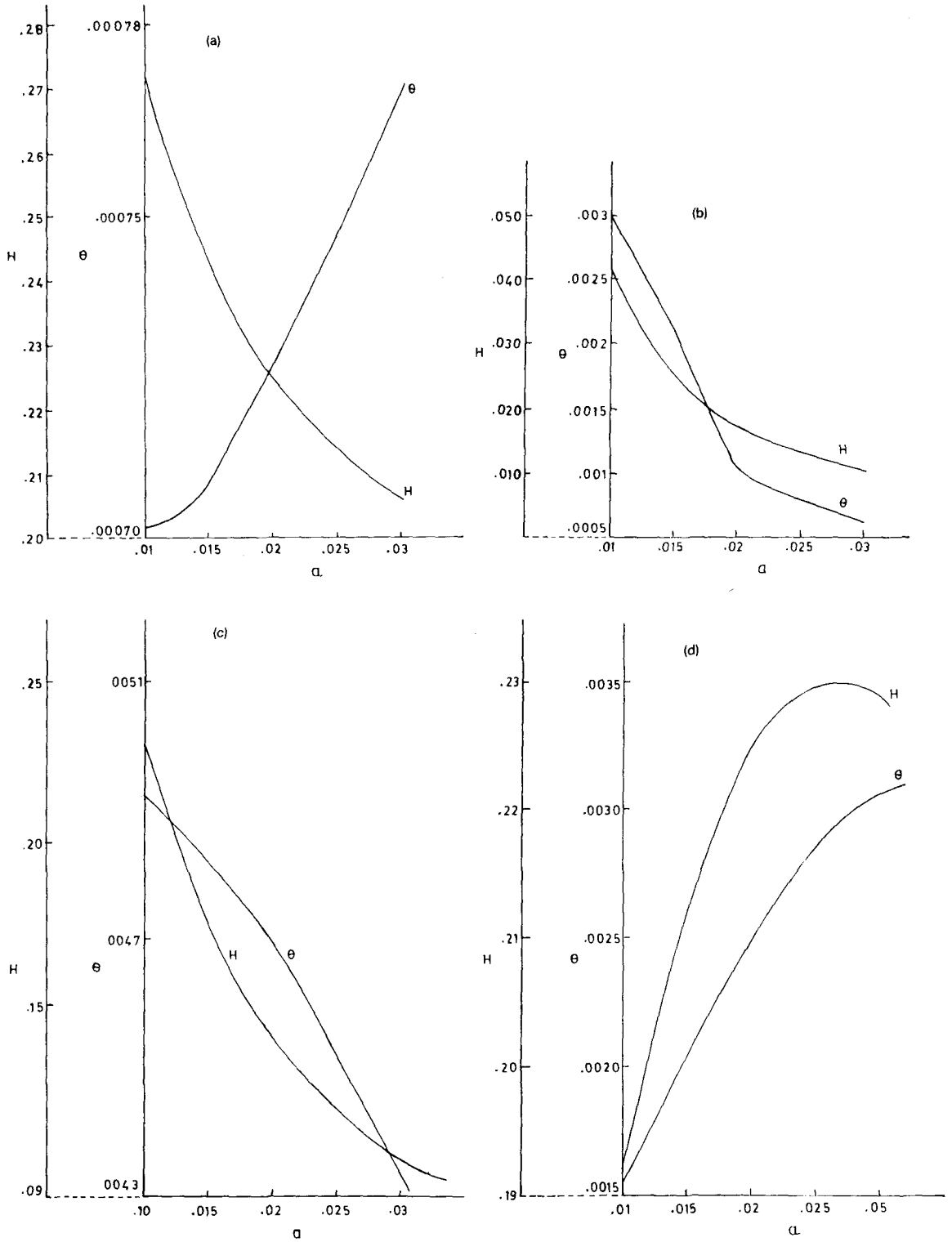

Figure 7. The plots of H vs. a and θ vs. a, when equation (8) is used as mapping function on the input images of (a) Figure 3, (b) Figure 4, (c) Figure 5, (d) Figure 6.

sense that its ambiguity will be greater for any other value of a.

Figure 7(a) implies that as a increases the Lincoln image possesses less ambiguity in level but has more spatial ambiguity. It therefore appears that the Lincoln and Cell images do not possess any valley. This indicates that optimal enhancement is not at all possible for them when one decides to use equaiton (8) as enhancement (mapping) function. To demonstrate the above facts the pictorial outputs for all the input images are shown in Figures 14(a)–(d) for a typical set of values of a.

Since the Lincoln and Cell images do not show any valley in any of the said measures, we have included two enhanced versions for each of them corresponding to lowest and highest ambiguity values. For the Chromosome and Biplane images

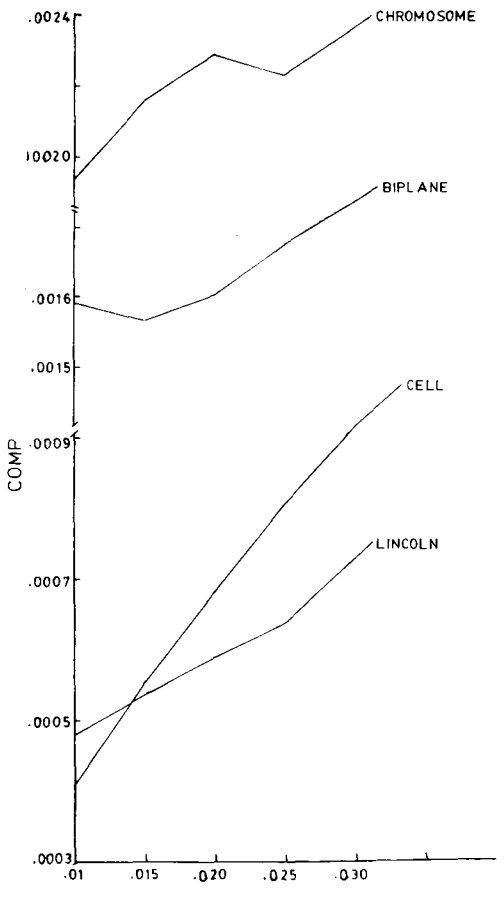

Figure 8. The plot of comp vs. a, when equation (8) is used as mapping function on the images of Figures 3–6.

the enhanced versions corresponding to the optimum value of a and two other values around it are shown.

Let us consider for example, the enhanced images of Chromosome (Figure 14(b)). Here the enhanced image other than the optimal one is either blurred (Chromosome boundary is not sharp) or disconnected. Similarly, for the Biplane image equation (8) with a value of a less than the optimal one is not able to discriminate the object from the background. On the other hand, the enhanced version corresponding to a value of a higher than the optimal one has resulted in fragmentation (decrease in homogeneity) within the object.

Figures 9(a)–(d) show the plots of $H(X)$ vs. D and $\theta(X)$ vs. D. Figure 10 shows the plots of comp(X) vs. D for equation (10) (Figure 2(c)). For each value of D the corresponding values of A, B and C are given in Figure 2(c). Figures 9(a), 9(b) and 9(c) corresponding to the input images Lincoln, Chromosome and Cell show distinct valleys in each case. On the other hand, both the curves of H and θ in Figure 9(d) show monotonically increasing behaviour with D. Their compactness measure (Figure 10) possesses a valley only for the Cell and Biplane images. Therefore, the transformed versions of the Lincoln, Chromosome, Cell and Biplane images corresponding all to $D = 13$ can be considered as optimal enhancement as far as H and θ, H and θ, H, comp and θ, and comp respectively are concerned.

Figures 15(a)–(d) demonstrate some of the enhanced outputs at and around $D = 13$ in order to exemplify the significance of the optimal version. It is to be noted from Figures 14(b) and 15(b) that the Chromosome image corresponding to $a = 0.025$ is optimum in the sense of compactness measure only, whereas the one in Figure 15(b) corresponding to $D = 13$ is optimum considering both H and θ. That is why the latter one is more acceptable than the former version as far as quality enhancement is concerend. Let us further consider Figures 14(d) and 15(d) where the optimal versions correspond to $a = 0.015$ and $D = 13$ considering only the compactness measure. The absolute value of compactness being lower in case of Figure 15(d) indicates its greater acceptability as enhanced version. This is also supported visually.

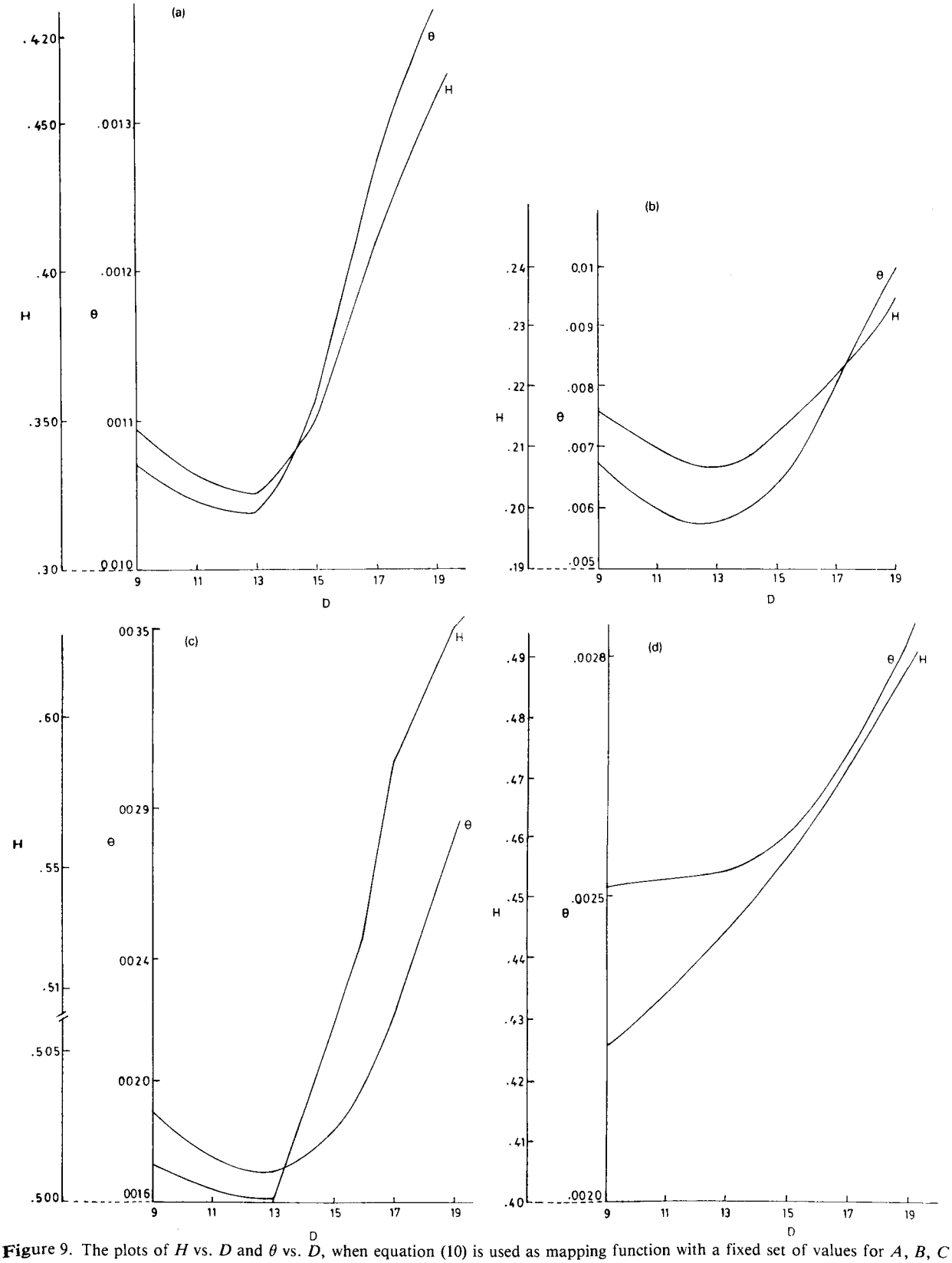

Figure 9. The plots of H vs. D and θ vs. D, when equation (10) is used as mapping function with a fixed set of values for A, B, C (for each value of D) and applied on the images of (a) Figure 3, (b) Figure 4, (c) Figure 5, (d) Figure 6.

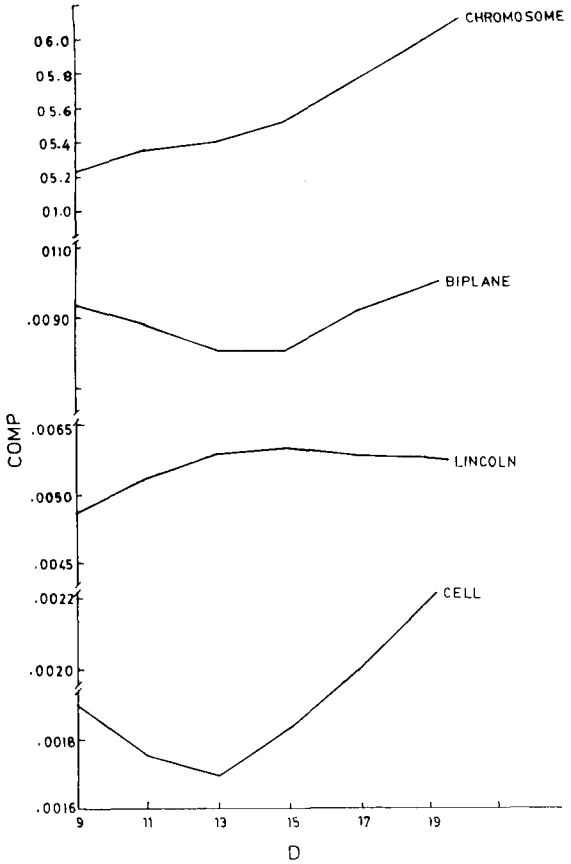

Figure 10. The plot of comp vs. D, when equation (10) is used as mapping function and applied on the images of Figures 3-6.

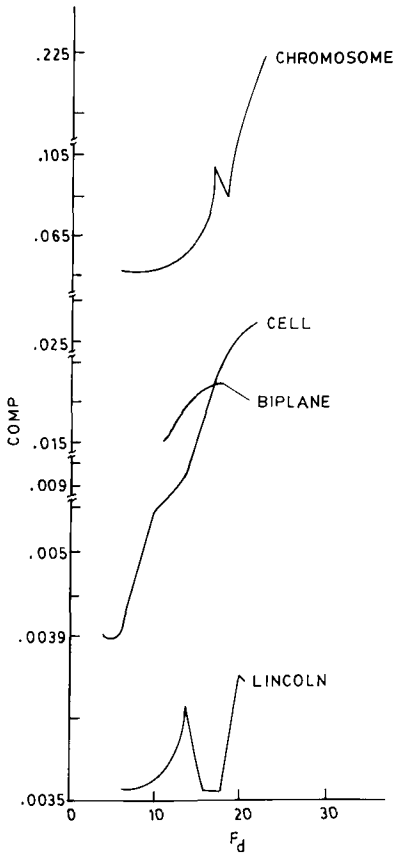

Figure 12. The plot of comp vs. F_d when equation (11) is used as mapping function ($F_e = 8$) and applied on the images of Figures 3-6.

The variation of H and θ with F_d of equation (11) (Figure 2(d)) corresponding to all the input images is shown in Figures 11(a) and 11(b). Here F_e is kept constant (at a value of 8) so that only the cross-over point will vary. Their compactness measures are plotted in Figure 12. It is seen that for the Lincoln image all the measures show the possibility of optimal enhancement around $F_d = 15$ ($F_d = 14$ for H and θ and $F_d = 18$ for comp). For the Biplane image H and θ provide a valley at $F_d = 17$. The Chromosome image possesses a valley only for the comp measure whereas the Cell image shows a valley only for the entropy measure. For demonstration we have included here only the enhanced outputs corresponding to the optimal F_d values. From Figure 16(a) it is seen that the enhanced Lincoln image corresponding to $F_d = 18$ looks better (discrimination of object from background) than that of $F_d = 14$. Comparing Figure 16(d) with the optimum versions of Figures 15(d) and 14(d) it is clearly visualized that Figure 16(d) minimizes both gray and spatial ambiguities whereas the other two minimize only the spatial ambiguity. A similar argument holds as well for the Chromosome and Cell images.

Figure 13 shows the plot of H vs. F_d when equation (12) is used as mapping function. For all the images, H is found to be monotonically decreasing and as expected, the minimum value obtained is always higher than that of the corresponding input images. This fact clearly indicates that there will be no enhancement at all by the function in equation (12). As a typical illustration of the said fact, we have included here only one transformed version

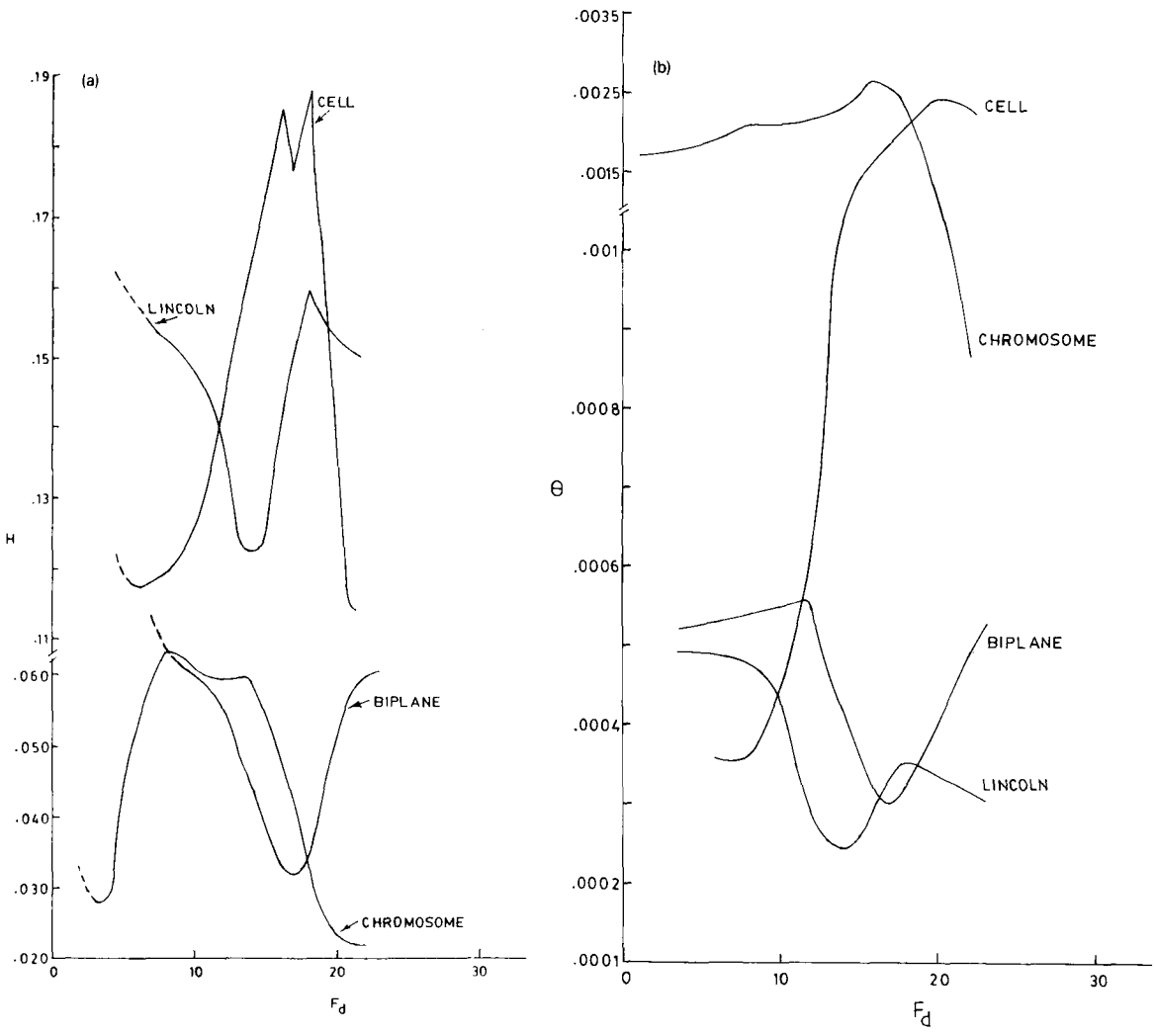

Figure 11. (a) The plot of H vs. F_d considering equation (11) as mapping function on the images of Figures 3-6 with $F_e = 8$. (b) The plot of θ vs. F_d considering equation (11) as mapping function on the images of Figures 3-6 with $F_e = 8$.

of the Lincoln image for $F_d = 22$ (Figure 17). As one can see, the contrast has decreased here as compared to the input image and a number of regions got merged.

The functional forms for optimal enhancement corresponding to the equations (8), (10) and (11) are found to satisfy the bounds described in Section 5.

For example, consider Figure 2(d) (equation (11)) where optimal enhancement functions correspond to the value of F_d lying in the range 14–18 and satisfy the bound conditions. Again, the function corresponding to $F_d = 12$ which gives no valley in variation of the fuzzy measures does not satisfy the bound criteria. Similarly, for Figures 2(a) and 2(c), the curves corresponding to $a = 0.1$ and 0.3, and $D = 17$ and 19 respectively do not lie within the bound functions.

Equation (12) (Figure 2(e)) has most of its variation at either end and almost no variation at the middle. This type of function is already found in [7] to be discarded (from the point of view of bounds) as mapping function in representing a fuzzy set. Figure 17 also corroborated this fact.

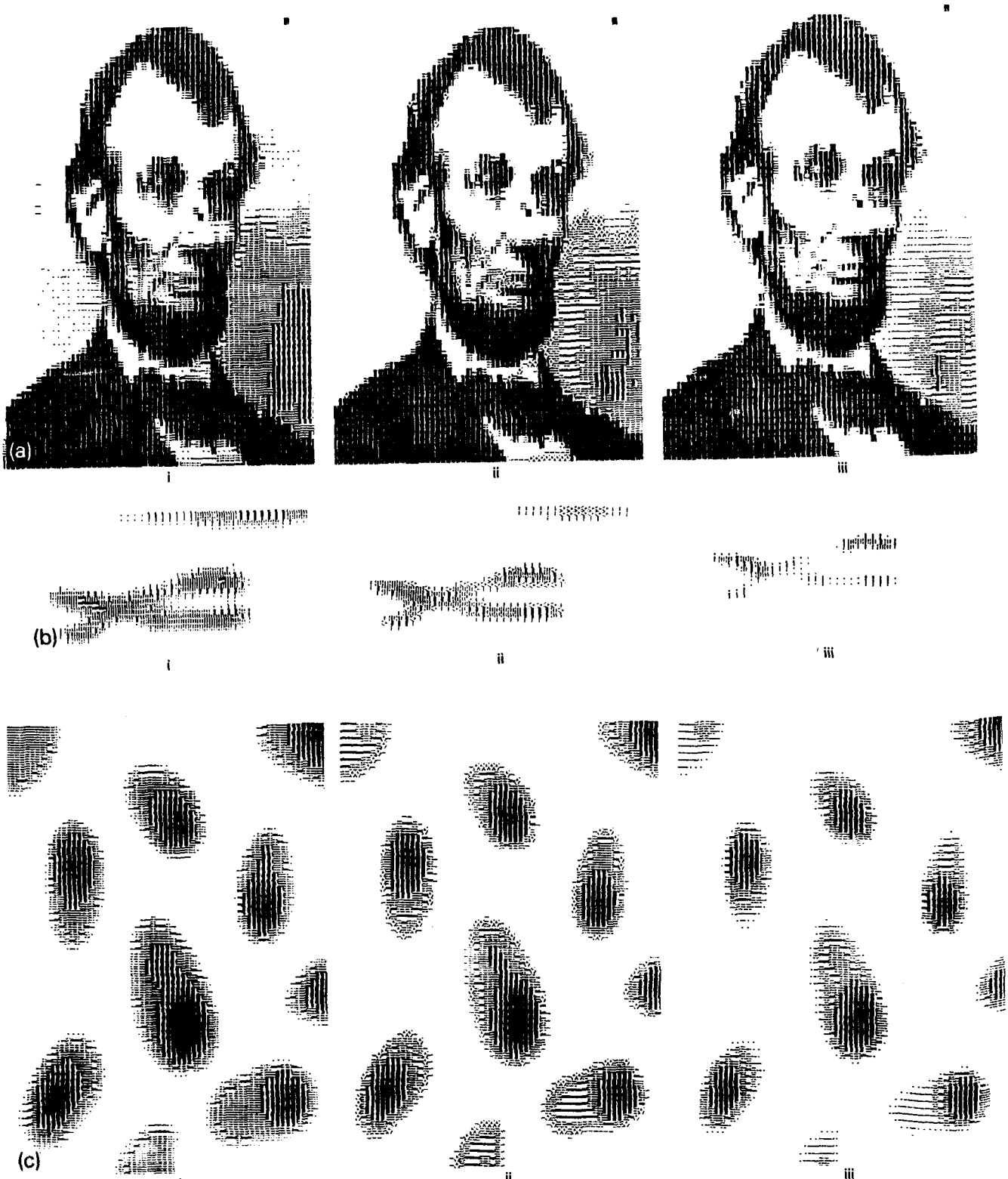
(a)
i
ii
iii
(b)
i
ii
iii
(c)
i
ii
iii

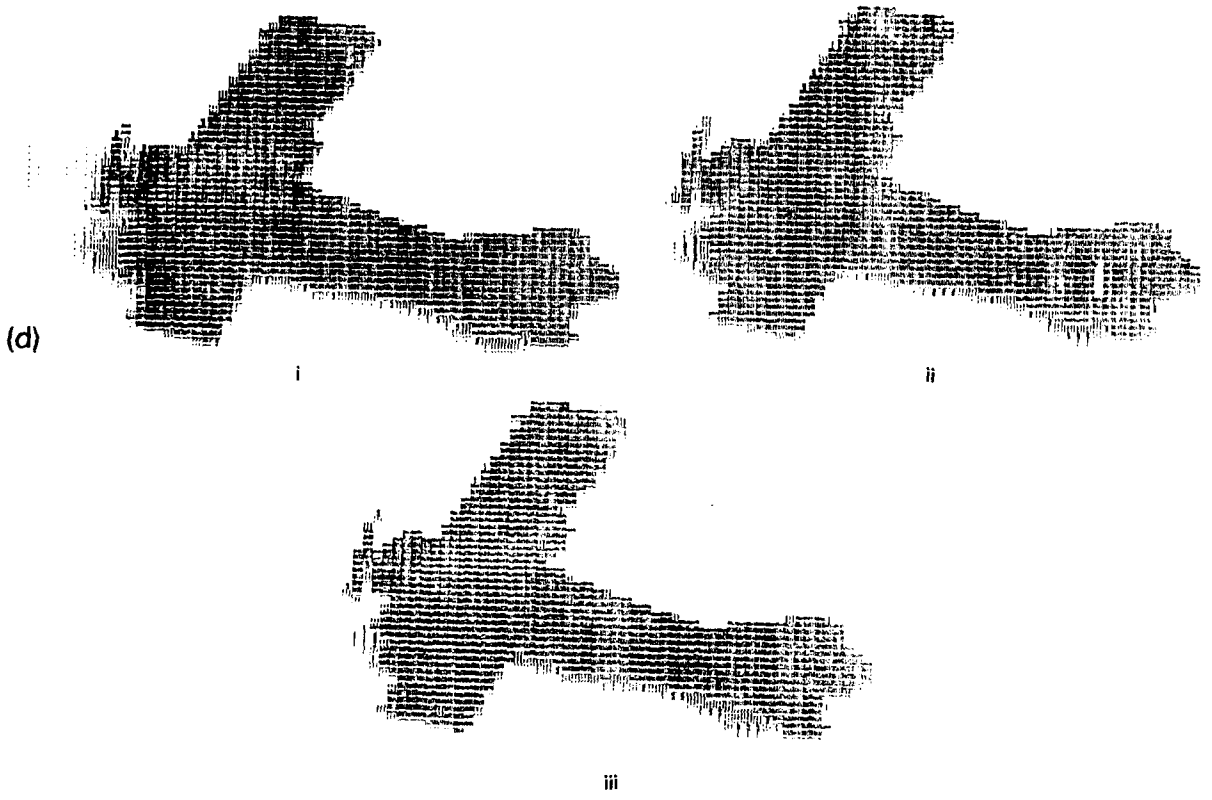

Figure 15. The transformed image output when equation (10) is used as mapping (enhancement) function on the input images of (a) Figure 3: (i) $D=11$ ($A=0.064$, $B=0.1$, $C=0.01$), (ii) $D=13$ ($A=0.074$, $B=0.15$, $C=0.01$), (iii) $D=17$ ($A=0.084$, $B=0.4$, $C=0.01$); (b) Figure 4: same A, B, C, D values as in Figure 15(a); (c) Figure 5: same A, B, C, D values as in Figure 15(a); (d) Figure 6: same A, B, C, D values as in Figure 15(a).

developed considering a single object in an image. Here we have considered single objects viz., Biplane and Chromosome, multiple objects like Cell and single objects with multiple disjoint regions such as Lincoln to demonstrate its effectiveness.

Functions like equations (10) and (11) are found to provide optimal enhancement for all types of images considered here as far as minimization of at least one of the fuzzy measures is concerned. For the Cell image its optimal enhancement produced by equation (10) is reflected by all the fuzzy measures. Similar is the case for the Lincoln image when equation (11) is considered. Visual discrimination of enhancement qualtiy produced by grayness am-

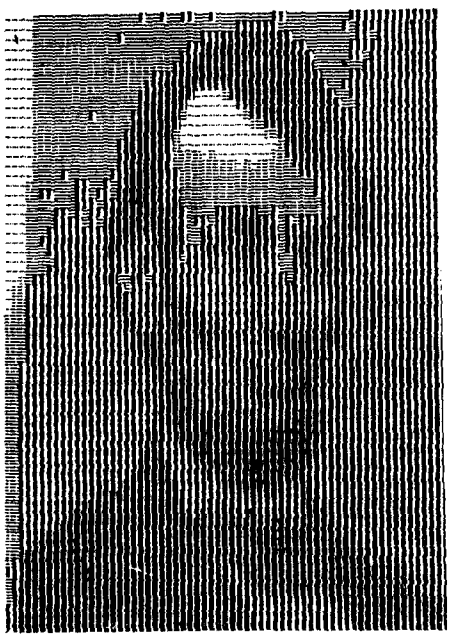

Figure 17. The transformed image output when equation (12) i used as mapping (enhancement) function in the Lincoln imag with $F_e=8$ and $F_d=22$.

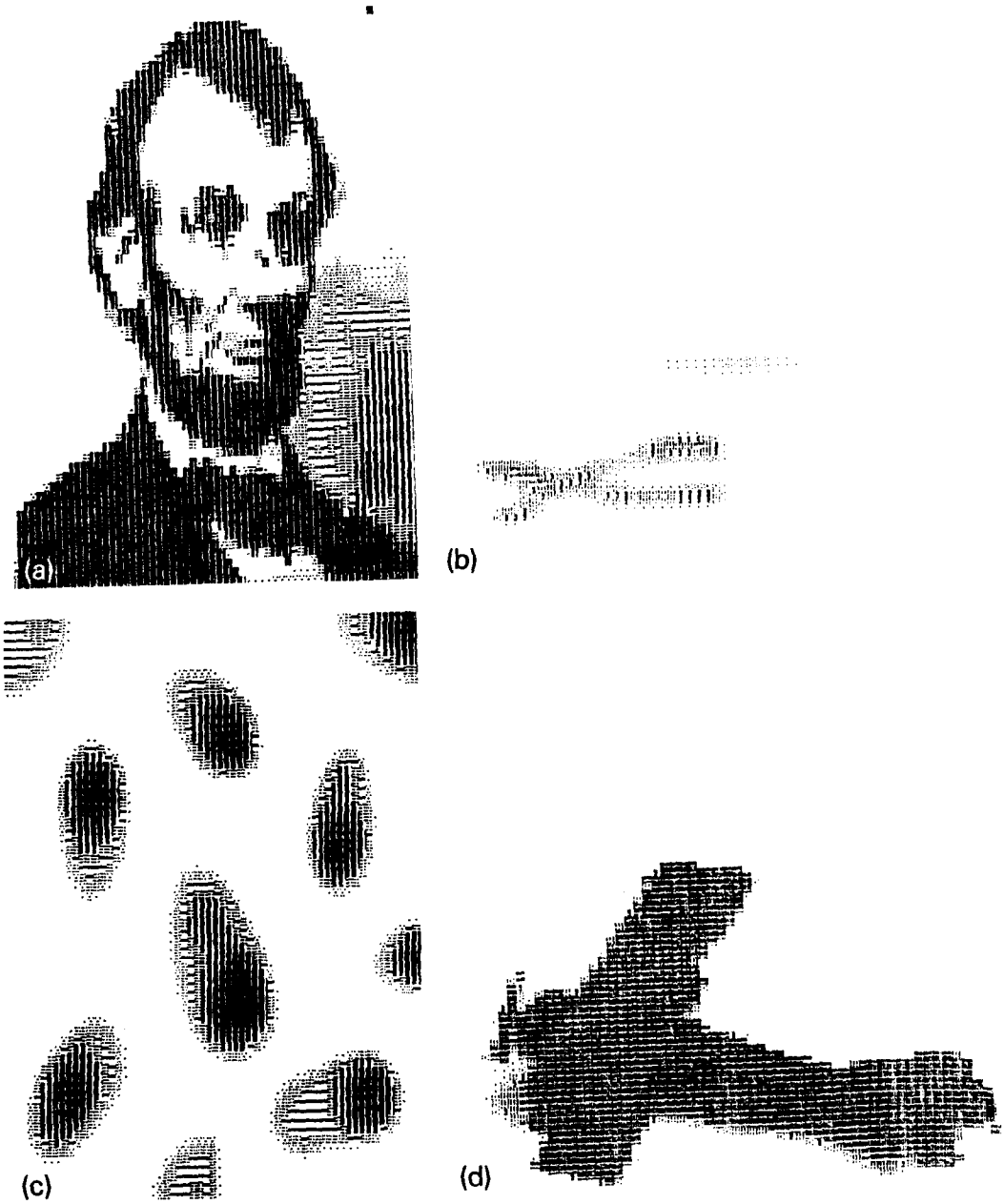

Figure 16. The transformed image output (optimum) when equation (11) is used as mapping (enhancement) function on Figures 3–6 (with $F_e = 8$): (a) $F_d = 16$, (b) $F_d = 18$, (c) $F_d = 18$, (d) $F_d = 17$.

biguity minimization and spatial ambiguity minimization is found to be well characterised by the respective measures.

Since the entropy (equation (2)) depends on the nature of the histogram of an image, a function like equation (10) (Figure 2(c)) was able to produce a valley in the behaviour of the H measure only for the images of Lincoln, Chromosome and Cell, because the appropriate selection of the parameter D made its cross-over point lie around thresholds between object and background. For the same reason, equation (11) (Figure 2(d)) has been able to

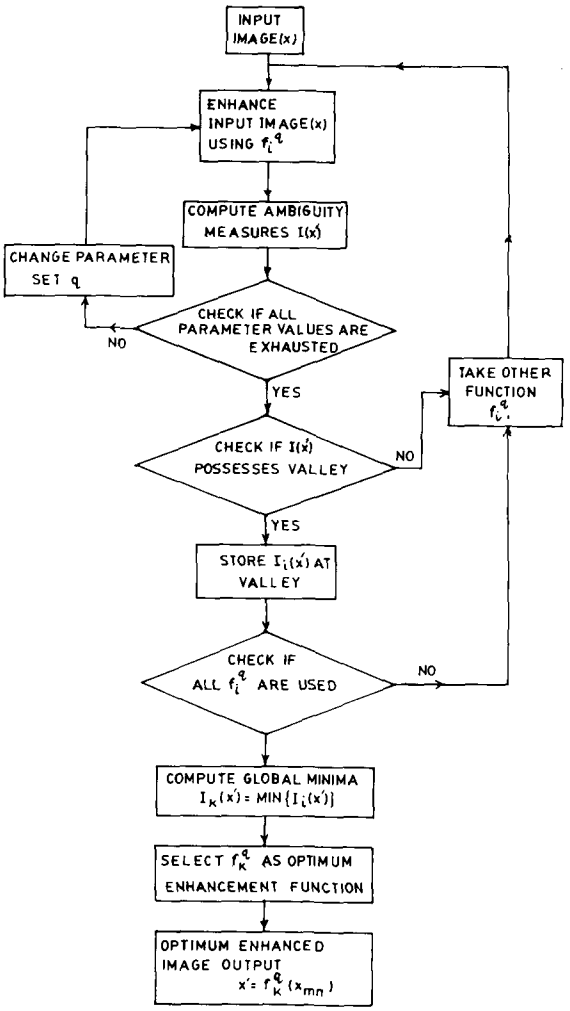

Figure 18. Block diagram of proposed algorithm.

produce a valley in the H measure for the Lincoln, Cell and Biplane images; the Chromosome image having a right skewed histogram got discriminated. However, minimizing both spatial and grayness ambiguity is a good indication for acceptance of an enhanced image.

Equation (8) showed comparatively inferior performance, because the test images do not have a left skewed histogram. Equation (12) increases the ambiguity in grayness of pixels and thus could not produce enhancement of any image. Bound functions are also found to be an indication for discarding enhancement functions.

It is to be mentioned here that four distinct enhancement functions have been considered here in order to cover most of the enhancement functions normally used [3]. All these functional forms can also be generated with only one function, namely, the standard beta density function [9] by changing its parameters.

Acknowledgement

The authors gratefully acknowledge Prof. D. Dutta Majumder for his interest in this work, Mr. S. Chakraborty for drawing the figures and Mr. J. Gupta for typing the manuscript. The facility provided by the DOE, Govt. of India for computing is also acknowledged.

References

[1] Gonzalez, R.C. and P. Wintz (1977). *Digital Image Processing*. Addison-Wesley, Reading, MA.

[2] Ekstrom, M.P. (1984). *Digital Image Processing Techniques*. Academic Press, New York.

[3] Wang, D.C.C., A.H. Vagnucci and C.C. Li (1983). Digital image enhancement: a survey. *Computer Vision, Graphics and Image Processing* 24, 368–381.

[4] Pal, S.K. and A. Rosenfeld (1988). Image enhancement and thresholding by optimization of fuzzy compactness. *Pattern Recognition Letters* 7, 77–86.

[5] Zadeh, L.A. (1975). Calculus of fuzzy restrictions. In: L.A. Zadeh et al., Eds., *Fuzzy Sets and Their Application to Cognitive and Decision Processes*. Academic Press, London, 1–39.

[6] Rosenfeld, A. (1984). Fuzzy geometry of image subsets. *Pattern Recognition Letters* 2, 311–317.

[7] Murthy, C.A. and S.K. Pal. Bounds for membership function: correlation based approach. *Fuzzy Sets and Systems*, submitted.

[8] Murthy, C.A., S.K. Pal and D. Dutta Majumder (1985). Correlation between two fuzzy membership functions. *Fuzzy Sets and Systems* 7 (1), 23–38.

[9] Tubbs, J.D. (1987). A note on parametric image enhancement. *Pattern Recognition* 20, 617–621.